Journal of Hazardous Materials 162 (2009) 469–475

Contents lists available at ScienceDirect

Journal of Hazardous Materials

journal homepage: www.elsevier.com/locate/jhazmat

Chemical and physical properties of plasma slags containing various amorphous volume fractions

Yi-Ming Kuo[a,*], Chih-Ta Wang[a], Cheng-Hsien Tsai[b], Lin-Chi Wang[c]

[a] *Department of Safety Health and Environmental Engineering, Chung Hwa University of Medical Technology, Tainan County 71703, Taiwan, ROC*

[b] *Department of Chemical and Materials Engineering, National Kaohsiung University of Applied Sciences, Kaohsiung 80778, Taiwan, ROC*

[c] *Department of Chemical and Materials Engineering, Cheng Shiu University, Kaohsiung 833, Taiwan, ROC*

ARTICLE INFO

Article history:
Received 26 February 2008
Received in revised form 14 May 2008
Accepted 14 May 2008
Available online 21 May 2008

Keywords:
Plasma torch
Basicity
Fly ash
Heavy metal
Immobilization

ABSTRACT

In this study, municipal solid waste incinerator fly ash was vitrified using a plasma torch. The fly ash contained rich Ca, causing a high basicity of 2.43. Pure quartz was used as an additive to adjust the basicity. BET surface area analysis, X-ray diffraction analysis, and a scanning electron microscope were used to examine the physical properties of slags. The chemical stability and the acid resistance of slags were evaluated using the toxicity characteristics leaching procedure and tests of acid bathing. The results indicate that the plasma torch effectively vitrified the fly ash. Anthropogenic metals with low boiling points, such as Cd, Pb, and Zn, were predominately vaporized into flue gas. Most of the metals with high boiling points, such as Cr, Cu, and Mn, remained in the slag. After the vitrification, hazardous metals were noticeably immobilized in all slags. However, the slags with higher amorphous volume fractions were more effective in metal immobilization and in resisting acid corrosion. This indicates that SiO_2 enhanced the formation of the glassy amorphous phase and improved the resistance of acid corrosion and the immobilization of hazardous metals.

1. Introduction

Incineration is a technology widely used for the treatment of municipal solid waste (MSW) in many industrialized countries due to the diminishing availability of landfill sites. In Taiwan, there are 23 incinerators with a total designed disposal capacity of 24,150 tons/day. In 2006, the total amounts of incinerated refuse and ashes (fly ash + bottom ash) in Taiwan were 5,683,000 and 1,026,000 tons, respectively [1]. Incinerated ashes potentially release toxic substances, such as polychlorinated dibenzo-*p*-dioxins (PCDDs), polychlorinated dibenzofurans (PCDFs), polycyclic aromatic hydrocarbons (PAHs), and heavy metal compounds, into the environment [2,3]. There are several technologies, including cement immobilization, acid extraction/sulfide stabilization, sintering, and vitrification, that can be used to properly dispose of the ashes [4–7]. Among these technologies, vitrification is energy consuming but effective in treating ashes [8]. In addition, it can also treat various hazardous materials such as fly ash, spent catalysts, sewage sludge, and radioactive waste [9–12]. It has been reported that using vitrification to treat incinerator ashes reduces the volume of wastes, immobilizes heavy metals, destroys organic toxics, and recovers valuable metals [13–15].

There are three kinds of energy sources for vitrification: electric melting, burner melting, and blast melting. Vitrification using a plasma torch is the most common in the electric melting type [16]. In a previous study, a plasma process successfully vitrified hazardous waste into an amorphous and stabilized slag [17]. During such a vitrification process, the mobility of hazardous metals was reduced and metals with low boiling points were mostly vaporized into the flue gas [15]. The leaching behavior of heavy metals and the crystalline characteristics in slags have been investigated in various types of vitrification. However, the chemical stability of slags has seldom been investigated.

The main object of this study is to investigate the physical and chemical characteristics of plasma slags. Fly ash from an incineration process was vitrified by a plasma torch. The crystalline and surface characteristics of slags were qualitatively examined and the leaching behavior of metals was evaluated. In addition,

---

[*] Corresponding author. Tel.: +886 6 2674567x854; fax: +886 6 2675049.
E-mail address: yiming@mail.hwai.edu.tw (Y.-M. Kuo).

0304-3894/$ – see front matter © 2008 Elsevier B.V. All rights reserved.
doi:10.1016/j.jhazmat.2008.05.074

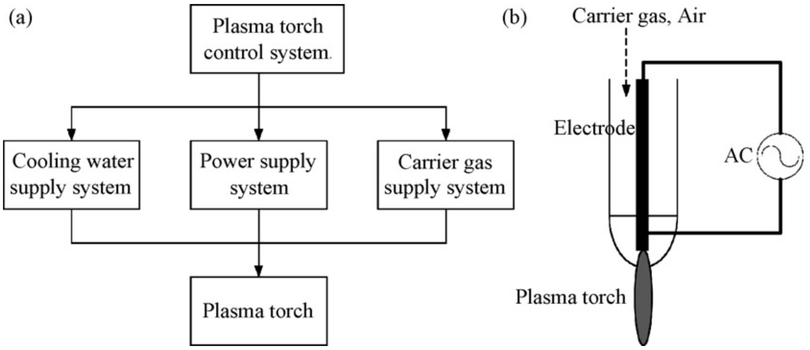

Fig. 1. Description of the plasma system: (a) components and (b) scheme of the plasma torch.

the correlation between the chemical stability and the amorphous glassy structure in slags was investigated.

2. Experimental

2.1. Sampling and vitrification

The fly ash used in this experiment was sampled from fabric filters in air pollution control devices at a MSW incinerator located in southern Taiwan. The unit in front of the fabric filters was a semi-dry scrubber with an injection of $Ca(OH)_2$ in a slurry form to remove gas acid pollutants. Crystallized SiO_2 (quartz) was added to adjust the basicity (mass ratio of CaO to SiO_2 before vitrification) of the fly ash with SiO_2/fly ash mass mixing ratios (S/A) of 0, 0.1, 0.2, 0.3 and 0.4. In a real scale plant, cullet or bottom ash serves as a source of Si because it is cost effective. However, there are many impurities in the additives which may interfere with the results. Hence, pure SiO_2 was used to avoid interference.

The ash mixtures were spindled into 10 g pellets and moistened using 1 mL ionized water to avoid being blown off by the carrier gas of the plasma system. The specimens were then vitrified by a non-transferred type of plasma torch operating at 2550 W for 20 min. Fig. 1 schematically depicts the non-transferred type of plasma torch which was used in this study. The internal electrode of the plasma torch was tungsten and the tip of the torch was copper. Argon, the carrier gas, metered at 1.0 L/min, was introduced into the system, with recirculated cooling water used as the cooling system for the plasma torch. The center temperature of the plasma torch was about 4000–10,000 °C. The vitrified slags were labeled as S-0–S-4 according to their S/A ratios, respectively. The metal composition and the mass loss of specimens were both determined to evaluate percent mass retained (mass retained in the slag/mass in the ash mixture, PMR) of the metal species after vitrification.

2.2. Estimation of metal content in specimens

The slags and fly ash were both pulverized to a particle size that passed through a mesh 100 sieve to ensure a consistent digestion efficiency. All 0.5 g samples were digested with an acid mixture ($1\,mL\ HBF_4 + 5\,mL\ HNO_3 + 5\,mL\ HClO_4$) in a hermetically sealed Teflon tube by a microwave digester. The heating program was: 20–180 °C at 10 °C/min and held isothermally for 30 min. The digestion solution was diluted to 25 mL with deionized water, filtrated by a cellulose ester filter, and then analyzed. An inductively coupled plasma atomic emission spectrometer (Jobin Yvon JY-38 Plus ICP-AES) was used to analyze the metal species, including Al, Ca, Cd, Cr, Cu, Fe, Mn, Pb, and Zn, in the sample digests to measure the metal composition of the slags and the fly ash. The relative composition of Si and Ca was determined using scanning electron microscopy–energy dispersive spectroscopy (JEOL JXA-840, SEM–EDS). The content of Ca was used to estimate the approximate mass fraction of Si in the specimens. The basicity of ash mixtures can be calculated using the following equation:

$$\text{basicity} = \frac{[\text{CaO}]}{[\text{SiO}_2]} = \frac{[\text{Ca}] \times (56/40)}{[\text{Si}] \times (60/28)}$$

[Ca] is the content of Ca (%) in the ash mixture before vitrification and [Si] is the content of Si (%) in the ash mixture before vitrification.

2.3. Evaluation of crystalline characteristics and amorphous phases of slags

The crystalline phases in slags were determined using X-ray diffraction (XRD) analysis. The analysis was carried out using a powder diffractometer (Geigerflex 3063) with Ni-filtered Cu Kα radiation on powders, at a particle size smaller than 20 μm, at $4^\circ\,\text{min}^{-1}$, in the $2\theta = 20$–60° range. Crystalline phases were identified by comparing intensities and positions of Bragg peaks with those listed in the Joint Committee on Powder Diffraction Standards (JCPDS) data files.

In this work, the volume fraction of the crystalline phase in slags was further measured with an XRD analysis using internal standard addition [18]. High-purity silica was mixed with specimens as an internal standard with a Si/sample mass ratio of 0.1. This served as a reference material in the crystalline quantitative analysis. The approximate fraction of the crystalline phase was then determined according to the area of the specific peaks in comparison with the internal standard. The details of the procedure are given in a

Table 1
Composition of fly ash and slag

Item	Crust metal (%)				Anthropogenic metal (mg/kg)					
	Al_2O_3[a]	CaO[a]	Fe_2O_3[a]	SiO_2[a]	Cd[a]	Cr[a]	Cu[a]	Mn[a]	Pb[a]	Zn[a]
Fly ash	0.604	19.4	1.63	7.97	36.8	508	300	285	2,520	7,320
S-0	0.793	28.0	2.20	17.6	9.07	1092	832	465	1,485	4,350
PRM (dimensionless)	0.768	0.844	0.790	1.29	0.144	1.26	1.62	0.954	0.345	0.348

[a] Species.

previous report [19]. The amorphous volume fractions (AVF) of slags were calculated using the following equation:

$$\mathrm{AVF} = 1 - \sum_{i=1}^{n} \mathrm{CP}_i$$

CP_i is the volume fraction of the ith crystalline phase.

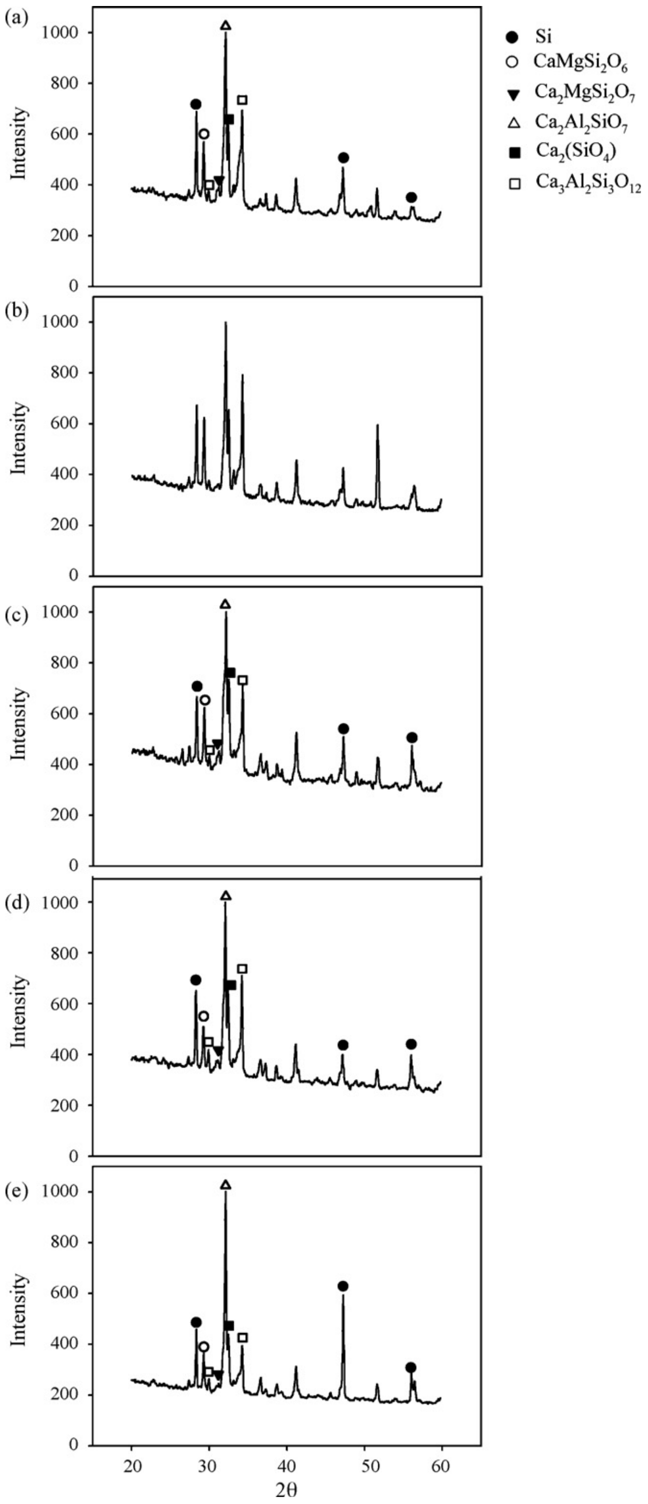

Fig. 2. XRD patterns of slags: (a) S-0, (b) S-1, (c) S-2, (d) S-3, and (e) S-4.

Table 2
Basicity, mass-specific BET surface, and AVF of specimens

Item	Basicity (dimensionless)	BET surface (m^2/g)	AVF (%)
Fly ash	–	5.03	–
S-0	2.43	0.154	38.5
S-1	1.87	0.644	43.3
S-2	0.990	0.090	48.6
S-3	0.674	0.585	56.1
S-4	0.511	0.089	70.2

2.4. Evaluation of the chemical stability and microstructure of specimens

The mobility of hazardous metal species in fly ash and slags was evaluated using the toxicity characteristic leaching procedure (TCLP). The extracts of TCLP were digested and diluted to a fixed volume following the detailed procedure given in Method 1311 [20]. In order to investigate the acid resistance of slags with various crystalline characteristics, the slags were pulverized and immersed in an acid solution of 3 wt% HCl for 7 days. The specimens were rinsed with deionized water and then dried at 105 °C for 1 h. The microstructures of the original and the acid-immersed slags were both qualitatively examined using a scanning electron microscope (SEM, Jeol JXA-840). Pulverized specimens (smaller than 74 μm) were adhered on a metallic plate, coated with Au using an ion sputter coater, and then scanned by the microscope. The concentrations of metal species in TCLP extracts and acid immersed solutions, including Cd, Cr, Cu, Mn, Pb, and Zn, were determined using atomic absorption spectrometry (SensAA, GBC).

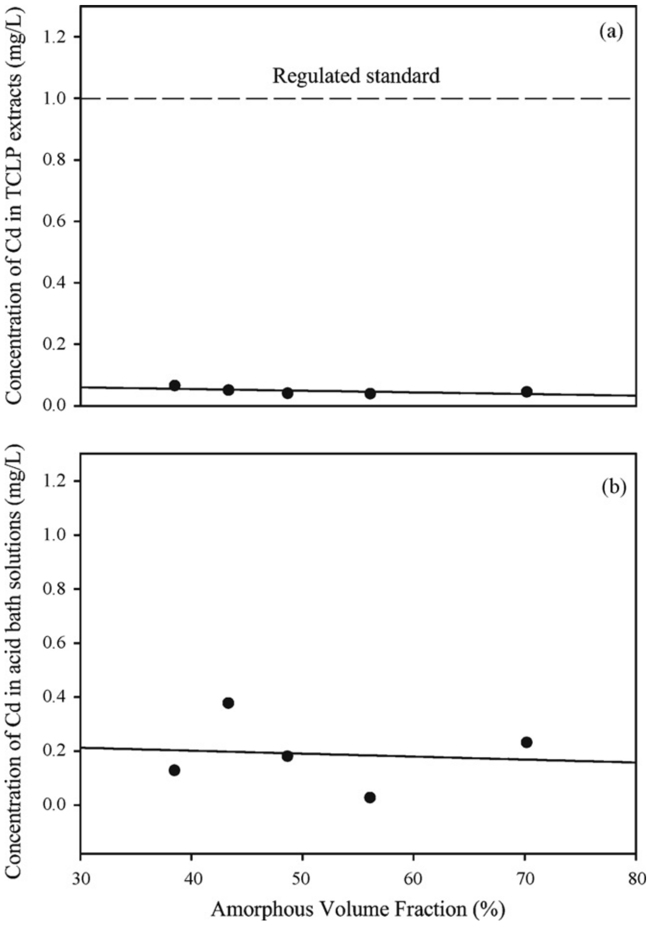

Fig. 3. Concentration of Cd in: (a) TCLP extracts and (b) acid immersing solutions.

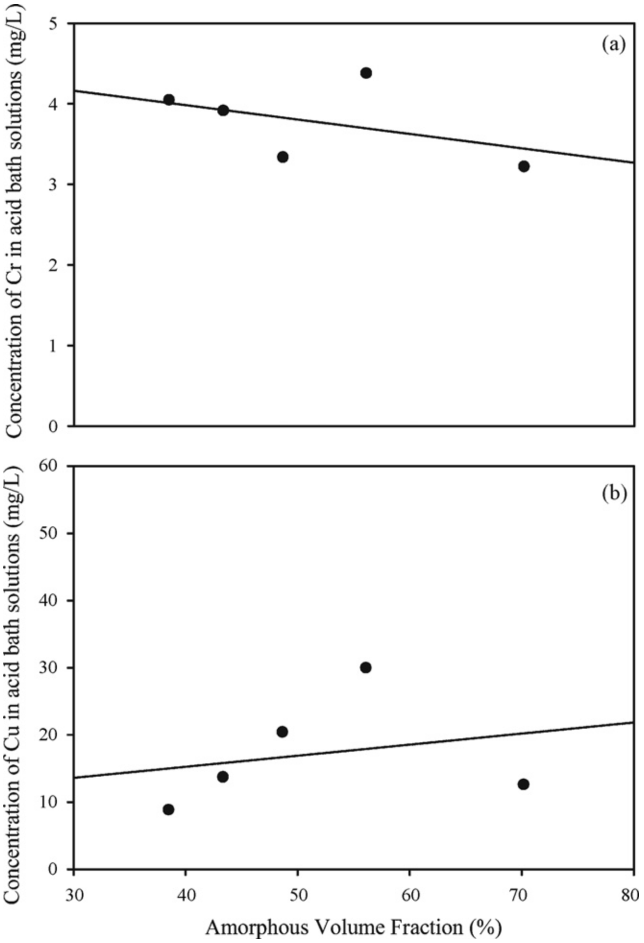

Fig. 4. Concentration of metals in acid immersing solutions: (a) Cr and (b) Cu.

3. Results and discussion

3.1. Composition of metal species in specimens

The fly ash was gray, powdery, and porous. After vitrification, the specimens with low S/A ratios were dark gray and had an uneven exterior. An increase in the S/A ratio made the slags gradually turn into dark green amorphous glasses. Table 1 illustrates the composition and PMR of metals in the fly ash and the slags. According to the toxicity, these metals can be divided into two categories: anthropogenic metals and crust metals, which are represented in elemental and oxide forms, respectively. The specimen of S-0 was used to represent other slags because the compositions of these slags were roughly similar, except for SiO_2, which was added during the vitrification. The ternary major glassy matrix elements, Al_2O_3, CaO, and SiO_2, made up 0.604, 19.4 and 7.97% of the fly ash, respectively and 0.793, 28.0, and 17.6% of S-0, respectively. The CaO content was extremely high in these specimens because the fly ash was sampled from the semi-dry scrubbers with the injection of $Ca(OH)_2$ to remove acidic pollutants in the flue gas. This also caused a high basicity of 2.43, which is not suitable to be directly vitrified without additives [21]. The major constituents of anthropogenic metals in the fly ash included: Cd (36.8 mg/kg), Cr (508 mg/kg), Cu (300 mg/kg), Mn (285 mg/kg), Pb (2520 mg/kg), and Zn (7320 mg/kg). After vitrification, the levels of Cr, Cu, and Mn were slightly elevated to 1090, 832, and 465 mg/kg, respectively. The mass reduction during vitrification caused these metals to be concentrated in the slags. The levels of Cd, Pb, and Zn were noticeably reduced to 9.07, 1485, and 4350 mg/kg, respectively. According to the results of PMRs, metals with low boiling points, like Cd, Pb, and Zn, were predominately vaporized into the flue gas [15]. The PMRs of these metals were higher than those from another vitrification process [20]. This is probably due to the relatively short vitrification time (20 min), which is considerably shorter than those in other processes. Therefore, there was insufficient time for Cd, Pb, and Zn to evaporate.

3.2. Crystalline and amorphous phases in slags

The XRD analysis patterns of the slags are shown in Fig. 2, on which the major crystalline phases are marked. The peaks at $2\theta = 28.4$, 47.2, and 56.1° are the peaks of Si, which was the internal standard. Other silicon-related phases, including diopside ($CaMgSi_2O_6$), akermanite ($Ca_2MgSi_2O_7$), gehlenite ($Ca_2Al_2SiO_7$), larnite (Ca_2SiO_4), and grossular ($Ca_3Al_2Si_3O_{12}$), were identified. These crystalline phases were slender or acicular in appearance and are commonly seen in igneous rocks. According to the XRD patterns of these slags, no new significant phases were found with an increase of added SiO_2.

Table 2 lists the basicity, mass-specific areas, and AVF of the specimens. The mass-specific areas of slags, ranging from 0.089 to 0.644 m^2/g, were one-order of magnitude lower than that of the fly ash (5.03 m^2/g). This indicates that the pores in the fly ash were filled and sealed during the vitrification. These results are consistent with the appearance of the specimens. The addition of SiO_2 gradually changed the basicity from 2.43 to 0.511 and caused the

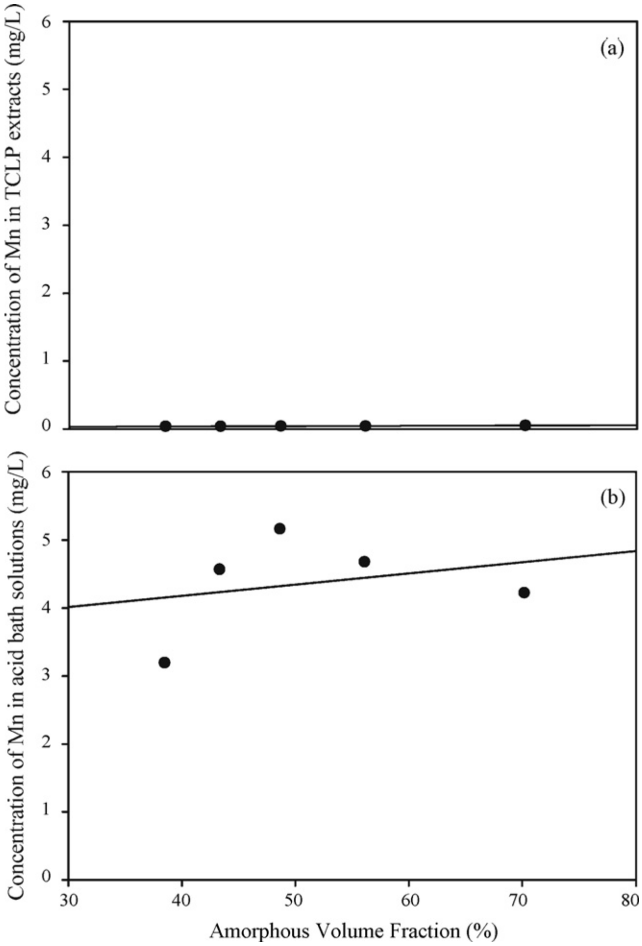

Fig. 5. Concentration of Mn in: (a) TCLP extracts and (b) acid immersing solutions.

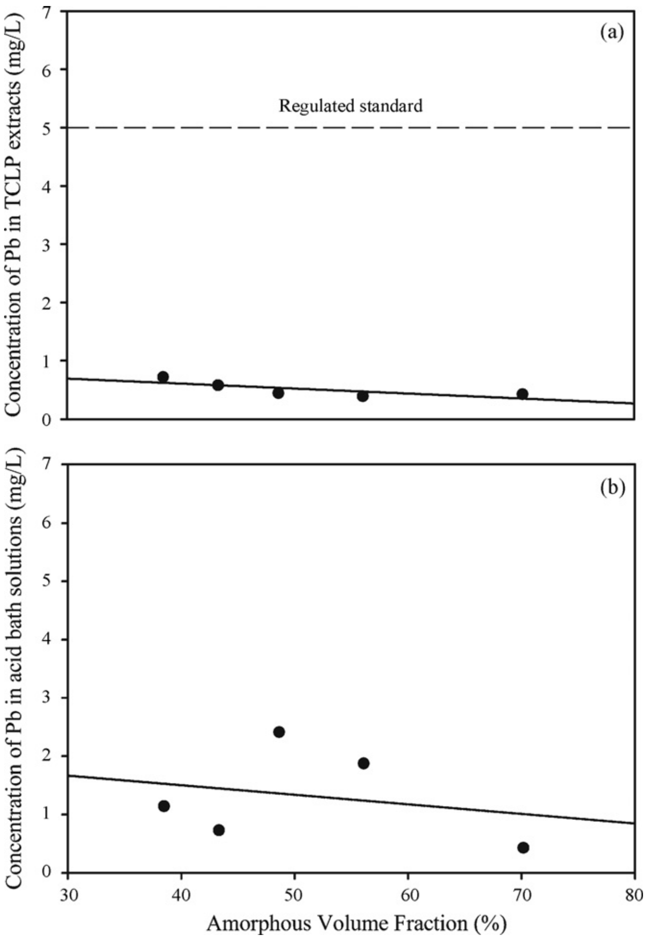

Fig. 6. Concentration of Pb in: (a) TCLP extracts and (b) acid immersing solutions.

AVF to increase from 38.5 to 70.2%. According to results of the XRD analysis and the estimation of AVF, the addition of SiO_2 caused an increase of AVF but did not cause the formation of a new crystalline phase in the plasma vitrification process. In our previous study, the adequate addition of SiO_2 in a melting process enhanced the transformation of crystalline phases and caused the formation of a glassy amorphous phase [22]. For the corresponding vitrification process, the fly ash was heated to 1400 °C by electricity, held for 2 h, and then cooled. There is a noticeable difference between the formations of crystalline phases in the slags from the two-vitrification processes. The most probable governing factors are the duration and temperature of vitrification.

3.3. Metal leaching behavior of slags

Figs. 3–7 illustrate the concentration of metals in extracts of TCLP and acid immersion. For Cd, the TCLP results were all below 0.1 mg/L and the concentration in the acid bath solution ranged between 0.028 and 0.378 mg/L. No significant relationship between the Cd leaching concentration and AVF was observed. The Cr and Cu concentrations in TCLP extracts were all below detection limits, so the corresponding figures are not shown. The concentrations of Cr in the acid bath solutions were about 4 mg/L. The values were slightly reduced in the slags containing higher AVF. For Cu, the concentrations in the acid bath solutions ranged from 10 to 40 mg/L, with no significant correlation between the Cu concentration and AVF. This shows that Cr and Cu were immobilized after vitrification, but slags with higher AVF were not more effective in encapsulating them.

In Fig. 5, the concentrations of Mn were all lower than 0.05 mg/L in TCLP extracts and were about 4 mg/L in the acid bath solutions. No significant trends were observed with a variety of AVF values. In Fig. 6, the concentration of Pb ranged from 0.393 to 0.712 and 0.429 to 2.41 mg/L in TCLP extracts and acid bath solutions, respectively. For Zn, the concentrations of TCLP extracts were all below 0.1 mg/L. The Zn concentration in acid bath solutions ranged from 50 to 150 mg/L. The leaching results of Pb and Zn show that slags with higher AVF potentially offer better immobilization of these two metals.

The Taiwanese regulated standards for heavy metals in a TCLP solution are Cd (1 mg/L), Cr (5 mg/L), Cu (15 mg/L), and Pb (5 mg/L) and the TCLP results of the slags are all below these limits [23]. For TCLP tests, slags with higher AVF offered better encapsulation of Pb and Zn, but not of the other metal species. When the slags were immersed in a strong acid, higher AVF also showed a noteworthy effect on the immobilization of Cr, Pb, and Zn. The mobility of heavy metals was reduced by vitrification; slags with higher AVF can further immobilize heavy metals in a glassy amorphous matrix with a better ability to resist acid attacks.

3.4. Microstructure and acid resistance of slags

Fig. 8 shows the microstructure of the plasma slags. A large number of acicular crystalline structures are clearly visible on the surface of all specimens. With more added SiO_2, bulks of amorphous glassy matrix started to form and the crystalline phases were reduced in quantity and became embedded inside the amorphous phase, but the shape of the crystalline phases remained acicular.

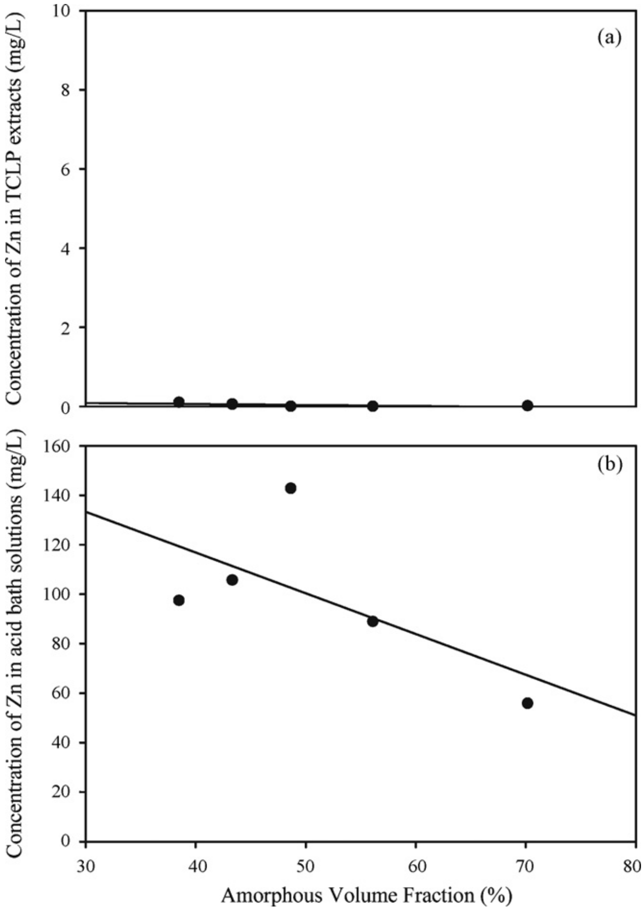

Fig. 7. Concentration of Zn in: (a) TCLP extracts and (b) acid immersing solutions.

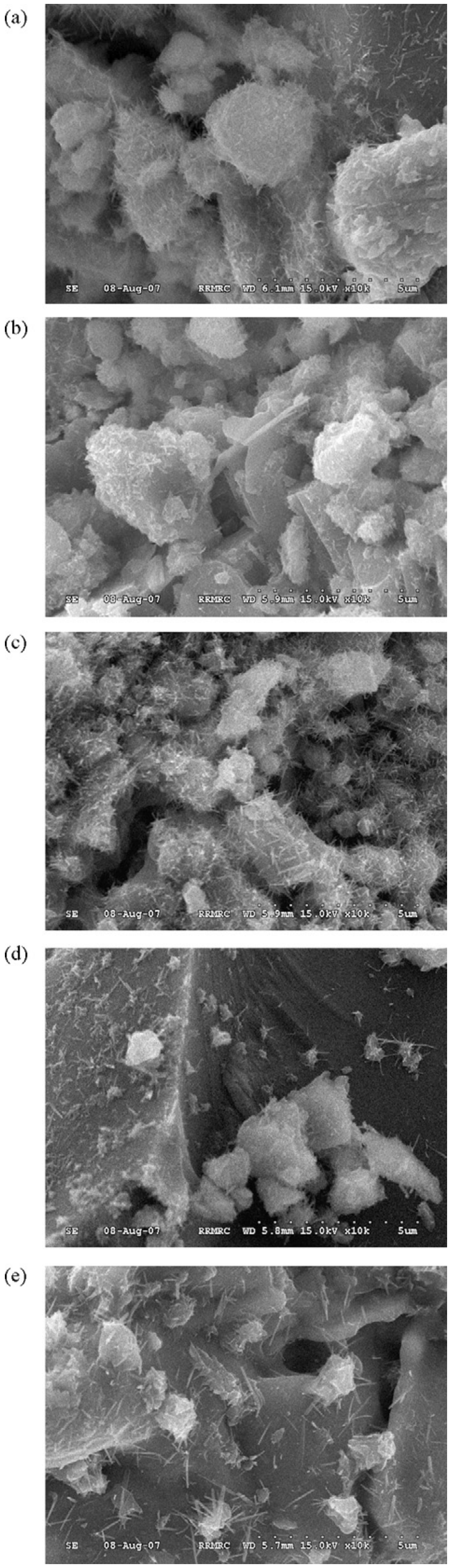

Fig. 8. Morphology of slags: (a) S-0, (b) S-1, (c) S-2, (d) S-3 and (e) S-4.

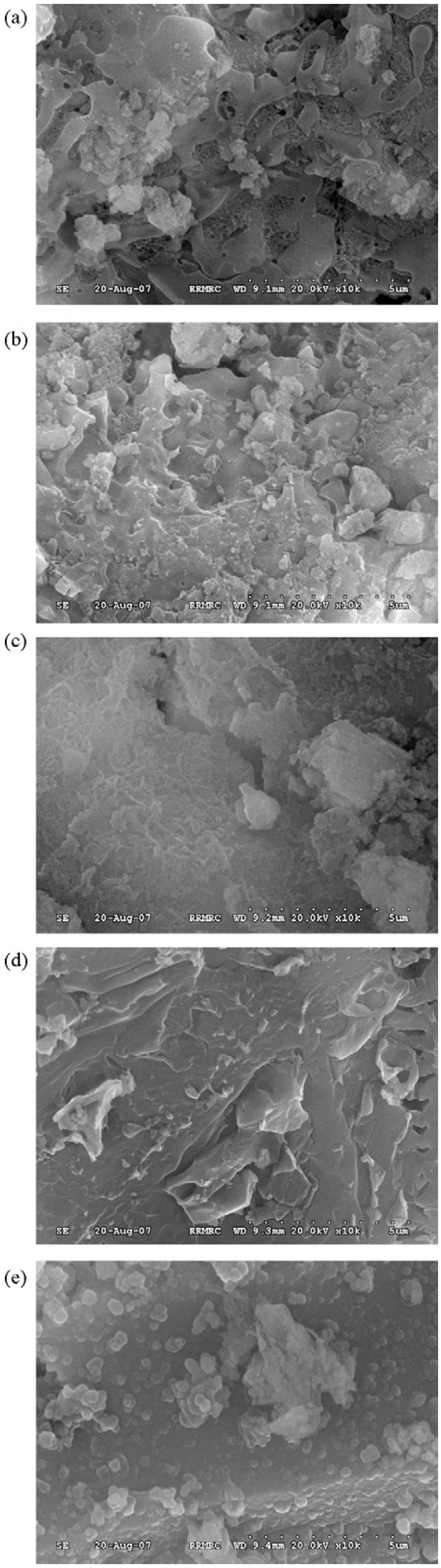

Fig. 9. Morphology of acid immersed slags: (a) S-0, (b) S-1, (c) S-2, (d) S-3 and (e) S-4.

This implies that the addition of SiO_2 enhanced the formation of a glassy amorphous phase but did not cause a transformation of the crystalline phase. The SEM images of the crystalline phases and the amorphous phases agree with the results of XRD analysis. Fig. 9 shows the microstructure of slags after acid bathing. In these SEM images, no acicular crystalline phases are present, but signs of corrosion or porous powder were observed on the surface of the specimens. This shows that the glassy amorphous phase had better acid resistance than did the crystalline phase.

4. Conclusion

The results show that a plasma torch effectively vitrified fly ash into an inert slag. The specific surfaces of slags were reduced to a magnitude of about 1/10. The major ternary constituents of the slag matrix were Al_2O_3 (0.604%), CaO (19.4%), and SiO_2 (7.97%). Anthropogenic metals with low boiling points, such as Cd, Pb, and Zn, were predominately vaporized into flue gas. Most of the metals with high boiling points, such Cr, Cu, and Mn, remained in the slag. The XRD analysis shows that the addition of SiO_2 during plasma vitrification increases the AVF in slags but does not cause the formation of new crystalline phases. After the vitrification, the mobility of hazardous metals was significantly reduced in slags containing either high or low AVF. In the tests of acid bathing, the slags with higher AVF were more effective in metal immobilization and in resisting acid corrosion. The SEM images of slags show that a glassy amorphous phase had better acid resistance, which also verifies that TCLP leaching and acid bath concentrations are relatively lower in slags with higher AVF. Therefore, the addition of SiO_2 during plasma vitrification enhanced the formation of a glassy amorphous phase and improved the acid resistance and the immobilization of hazardous metals.

References

[1] Environmental Protection Administration, Executive Yuan, Taiwan, Yearbook of Environmental Protection Statistics, 2007.

[2] A. Yasuhara, T. Katami, Leaching behavior of polychlorinated dibenzo-*p*-dioxins and furans from the fly ash and bottom ash of a municipal solid waste incinerator, Waste Manage. 27 (2007) 439–447.

[3] P. Sun, L.K. Weavers, P. Taerakul, H.W. Walker, Characterization of polycyclic aromatic hydrocarbons (PAHs) on lime spray dryer (LSD) ash using different extraction methods, Chemosphere 62 (2006) 265–274.

[4] P. Chindaprasirt, P. Kanchanda, A. Sathonsaowaphak, H.T. Cao, Sulfate resistance of blended cements containing fly ash and rice husk ash, Construct. Build. Mater. 21 (2007) 1356–1361.

[5] H. Katsuura, T. Inoue, M. Hiraoka, S. Saika, Full-scale plant study on fly ash treatment by the acid extraction process, Waste Manage. 16 (1996) 491–499.

[6] T. Mangialardi, Sintering of MSW fly ash for reuse as a concrete aggregate, J. Hazard. Mater. B87 (2001) 225–239.

[7] Y.M. Kuo, T.C. Lin, P.J. Tsai, Immobilization and encapsulation during vitrification of incineration ashes in a coke bed furnace, J. Hazard. Mater. B133 (2006) 75–78.

[8] L. Reijnders, Disposal uses and treatments of combustion ashes: a review, Resour. Conserv. Recycl. 43 (2005) 313–336.

[9] Y.M. Kuo, T.C. Lin, P.J. Tsai, Effect of SiO_2 on immobilization of metals and encapsulation of a glass network in slag, J. Air Waste Manage. 53 (2003) 1412–1416.

[10] Y.L. Wei, Y.Y. Lin, J.Q. Yang, H.P. Wang, T.L. Hsiung, Effect of plasma treatment on Ni molecular environment in a spent catalyst and a plating sludge, J. Electron. Spectrosc. Relat. Phenom. 156–158 (2007) 232–235.

[11] P. Kanchanapiyaa, T. Sakanoa, C. Kanaokab, T. Mikunia, Y. Ninomiyac, L. Zhangc, M. Masuid, F. Masamia, Characteristics of slag, fly ash and deposited particles during melting of dewatered sewage sludge in a pilot plant, J. Environ. Manage. 79 (2006) 163–172.

[12] L.S. Pioro, B.F. Sadovskiy, I.L. Pioro, Research and development of a high-efficiency one-stage melting converter-burial-bunker method for vitrification of high-level radioactive wastes, Nucl. Eng. Des. 205 (2001) 133–144.

[13] H. Ecke, H. Sakanakura, T. Matsuto, N. Tanaka, A. Lagerkvist, Effect of electric arc vitrification of bottom ash on the mobility and fate on metals, Environ. Sci. Technol. 35 (2001) 1531–1536.

[14] Y.M. Kuo, T.C. Lin, P.J. Tsai, W.J. Lee, H.Y. Lin, Fate of polycyclic aromatic hydrocarbons during vitrification of incinerator ash in a coke bed furnace, Chemosphere 51 (2003) 313–319.

[15] Y.M. Kuo, T.C. Lin, P.J. Tsai, Metal behavior during vitrification of incinerator ash in a coke bed furnace, J. Hazard. Mater. B109 (2004) 79–84.

[16] E. Ecke, H. Sakanakura, T. Matsuto, N. Tanaka, A. Lagerkvist, State-of-the-art-treatment processes for municipal solid waste incineration residues in Japan, Waste Manage. Res. 18 (2000) 41–51.

[17] K. Moustakas, D. Fatta, S. Malamis, K. Haralambous, M. Loizidou, Demonstration plasma gasification/vitrification system for effective hazardous waste treatment, J. Hazard. Mater. B123 (2005) 120–126.

[18] B.D. Cullity, S.R. Stock, Elements of X-ray Diffraction, 3rd ed., Prentice Hall, Upper Saddle River, 2001.

[19] Y.M. Kuo, J.W. Wang, C.H. Tsai, Encapsulation behaviors of metals in slags containing various amorphous volume fractions, J. Air Waste Manage. 57 (2007) 820–827.

[20] Environmental Protection Administration of United States Toxicity Characteristic Leaching Procedure: SW846 Method 1311.

[21] Y.M. Kuo, J.W. Wang, H.R. Chao, C.T. Wang, G.P. Chang-Chien, Effect of cooling rate and basicity during vitrification of fly ash. Part 2. On the chemical stability and acid resistance of slags, J. Hazard. Mater 152 (2008) 554–562.

[22] Y.M. Kuo, J.W. Wang, C.T. Wang, C.H. Tsai, Effect of water quenching and SiO_2 addition during vitrification of fly ash. Part 1. On the crystalline characteristics of slags, J. Hazard. Mater. 152 (2008) 994–1001.

[23] Environmental Protection Administration, Executive Yuan, Taiwan, Standards for Defining Hazardous Waste 2006.